analytical chemistry

pubs.acs.org/ac

Article

AND Logic-Gate-Based CRISPR/Cas12a Biosensing Platform for the Sensitive Colorimetric Detection of Dual miRNAs

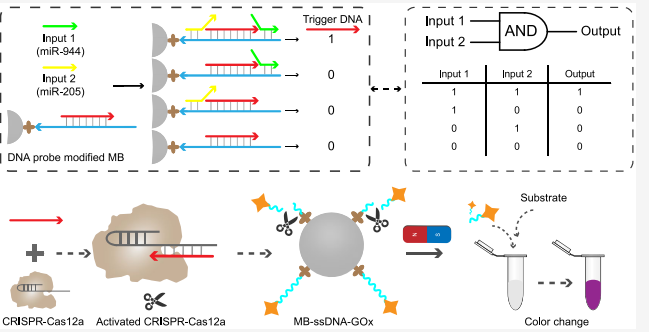
Shaohua Gong, Xi Wang, Ping Zhou, Wei Pan, Na Li,* and Bo Tang*

Cite This: https://doi.org/10.1021/acs.analchem.2c03666

Read Online

ACCESS | Metrics & More | Article Recommendations | Supporting Information

ABSTRACT: Clustered regularly interspaced short palindromic repeats (CRISPR)-Cas (CRISPR-associated) system has been widely explored for the detection of disease-related nucleic acids. Nevertheless, the simultaneous detection of multiple nucleic acids within one assay using the CRISPR-Cas system is still challenging. In this study, we develop an AND logic-gate-based CRISPR-Cas12a biosensing platform to achieve the sensitive colorimetric detection of dual miRNAs. Specifically, the DNA probe was designed to recognize the binary input of miRNAs and to output trigger DNA, which activated the CRISPR-Cas12a system to cut single-stranded DNA (ssDNA). The ssDNA on magnetic beads (MBs) was cleaved by the activated CRISPR-Cas12a, causing the separation of glucose oxidase (GOx) from MB and the subsequent generation of a colorimetric signal. The color change induced by 1 pM of target miRNAs can be directly distinguished by the naked eye and the instrumental limit of detection reaches 36.4 fM. The overexpressed miR-205 and miR-944 in the real human serum can be detected, allowing us to differentiate between lung cancer patients and healthy people. Furthermore, the developed strategy achieves simultaneous detection of dual miRNAs using CRISPR-Cas12a with one kind of crRNA, avoiding sophisticated nucleic acid amplifications and the use of bulky instruments. The current method can broaden the CRISPR-Cas12a-based applications for multiple biomarkers detection and precise disease diagnosis.



Downloaded via SHANGHAI NORMAL UNIV on November 3, 2022 at 09:22:54 (UTC).
See https://pubs.acs.org/sharingguidelines for options on how to legitimately share published articles.

Clustered regularly interspaced short palindromic repeats (CRISPR)-Cas (CRISPR-associated) system has emerged as a versatile and powerful technology for molecular diagnosis.[1−4] As a type of CRISPR-Cas system composed of CRISPR RNA (crRNA) and Cas12a nuclease, CRISPR-Cas12a can recognize different target DNAs using adjustable crRNA and subsequently nonspecifically cleaves single-stranded DNA (ssDNA).[5,6] This property endows CRISPR-Cas12a with the capability of signal amplification and makes it an excellent biosensing tool. Various strategies based on CRISPR-Cas12a have been reported for the detection of nucleic acids.[7−12] In these strategies, the target nucleic acid is directly recognized by CRISPR-Cas12a for signal generation, or it is first amplified with nucleic acid amplification methods (such as recombinase polymerase amplification, loop-mediated isothermal amplification) to produce amplicons, which are used to activate CRISPR-Cas12a for the collateral cleavage of ssDNA[13−16] However, CRISPR-Cas12a with specific crRNA can only recognize one kind of target nucleic acid. For the detection of multiple nucleic acids, which is important for an accurate diagnosis of diseases, various crRNAs need to be designed and assembled with Cas12a for the recognition of the corresponding target nucleic acids, leading to an increase in detection cost and complexity.[17−22] Therefore, it is desirable to develop a CRISPR-Cas12a-based strategy using only one kind of crRNA for the detection of multiple nucleic acids.

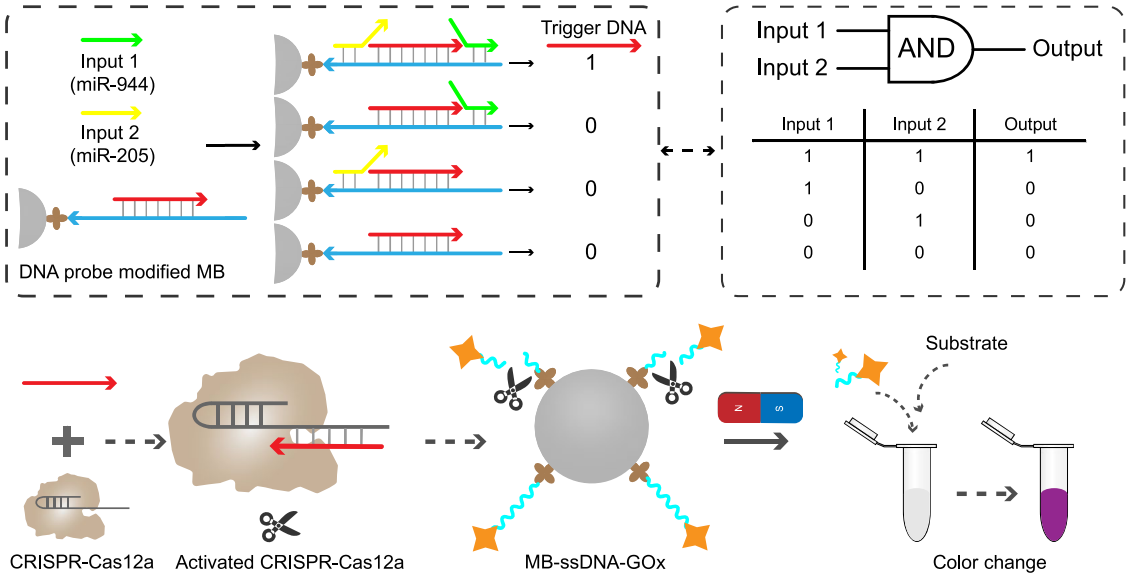
DNA computation uses logic gates as a module to process the input signal of biological molecules through DNA strand exchanges and to generate a controllable output signal.[23−25] On the basis of biomolecular programming capability, DNA computation has been applied for the detection of various biomolecules, such as small molecules, nucleic acids, and proteins.[26−28] The biomolecules can initiate DNA computation and lead to the output of ssDNA, which is labeled with a fluorophore or electrochemical tag for direct signal detection, or triggers downstream nucleic acid amplification reaction for more sensitive signal detection.[29−32] Notably, the output ssDNA can also serve as an initiator to activate the trans-cleavage activity of CRISPR-Cas12a for signal amplification. Thus, the combination of DNA computation and CRISPR-Cas12a can achieve simultaneous detection of multiple nucleic acids within one assay.

Herein, we established an AND logic-gate-based CRISPR-Cas12a biosensing platform for the sensitive colorimetric

Received: August 21, 2022
Accepted: October 21, 2022

ACS Publications © XXXX American Chemical Society

Scheme 1. Schematic Illustration of the Developed Strategy for the Colorimetric Detection of Dual miRNAs



detection of dual miRNAs. The occurrence of a disease is often accompanied by an abnormal expression of different miRNAs.[33] Also, the same miRNA is also possible to be aberrantly expressed in different diseases.[34−37] miR-944 and miR-205 have been reported to be overexpressed in lung cancer patients and thus are chosen as the model analytes.[38,39] Simultaneous detection of both miR-205 and miR-944 may contribute to the accurate diagnosis of lung cancer. In the developed platform, a DNA probe was rationally constructed and modified on magnetic beads (MBs) to recognize the binary inputs of miRNAs. In the absence of one kind of target miRNA, the output signal of the AND logic gate was 0 and no trigger DNA was generated. Only in the presence of the dual miRNAs, the output signal of the AND logic gate was 1 and the trigger DNA could be released. The trigger DNA initiated the trans-cleavage activity of CRISPR-Cas12a and enabled it to nonspecifically cut the ssDNA on MB. The cleavage of ssDNA resulted in the release of glucose oxidase (GOx) from the surface of MB because the ssDNA served as the linker for MB and glucose oxidase (GOx). After magnetic separation, MB was removed and the separated GOx was retained in the supernatant. The released GOx could catalyze the chromogenic substrate to generate a visible change in color (Scheme 1). The developed strategy that integrated CRISPR-Cas12a with the AND logic gate successfully realized signal processing of input nucleic acids and obvious colorimetric detection of 1 pM of target miRNAs by the naked eye.

EXPERIMENTAL SECTION

Preparation of ssDNA-Modified GOx. One OD of thiolated DNA was added with 30 μL of ultrapure water and 2 μL of NaH_2PO_4 buffer (1 M, pH 5.5). After that, 2 μL of tris(2-carboxyethyl) phosphine (TCEP) solution (200 mM) was added to activate the thiol for 1 h. The activated DNA was then purified by Amicon-3k with buffer A (0.1 M NaCl, 0.1 M sodium phosphate buffer, pH 7.3) five times. Eight milligrams of GOx and 1 mg of sulfosuccinimidyl-4-(*N*-maleimidomethyl) cyclohexane-1-carboxylate (sulfo-SMCC) were first dissolved in 300 μL of buffer A and 100 μL of buffer A, respectively. Then, the solution was mixed and shaken for 3 h at 30 °C to obtain the sulfo-SMCC-modified GOx. The superfluous insoluble sulfo-SMCC was removed by centrifugation. Finally, the sulfo-SMCC-modified GOx was purified by Amicon-100K with buffer A. The sulfo-SMCC-modified GOx and activated DNA were mixed and shaken for 48 h at 30 °C. After that, GOx-ssDNA was purified by Amicon-100K with PBS five times. The absorbance of the ssDNA-modified GOx (GOx-ssDNA) was measured at 280 nm on nanodrop one. Finally, the GOx-ssDNA was diluted with PBS and the absorbance of the solution at 280 nm was determined to be 1.

Preparation of GOx-Modified MB-SA. The supernatant of MB-SA (50 μL, 10 mg/mL) was removed. The obtained MB-SA was incubated with 50 μL of the obtained GOx-ssDNA solution for 1 h. The products were washed with PBST (PBS, 0.05% Tween 20) three times and eventually dispersed in 50 μL of PBST for further use.

Modification of DNA Probe on MB-SA. The concentrations of trigger DNA and long-strand DNA were diluted to 7.5 and 5 nM, respectively, with PBS. Next, 50 μL of the trigger DNA solution and 50 μL of the long-strand DNA solution was mixed for 30 min at room temperature. After that, the supernatant of MB-SA (25 μL, 10 mg/mL) was removed. Also, the obtained MB-SA was incubated with 500 μL of the above DNA mixture for 1 h. The unbound DNA was removed. The DNA probe-modified MB-SA was washed with PBST and dispersed in 25 μL of PBST for further use.

Quantification of Biotinylated DNA Modified on MB-SA. Twenty microliters of the biotinylated DNA solution was added with 2 μL of MB-SA (10 mg/mL). The mixture was incubated at room temperature for 30 min. After that, MB-SA was separated via magnetic separation. The decrease of biotinylated DNA was measured by a nanodrop one. The amount of biotinylated DNA modified on MB-SA was calculated by the equation: [(the initial biotinylated DNA concentration − the biotinylated DNA concentration in supernatant) × (the volume)]/(the mass of MB-SA). The biotinylated DNA strands modified on MB-SA was calculated by the formula: [(the initial biotinylated DNA concentration − the biotinylated DNA concentration in supernatant) × (the volume) × 6.02×10^{23}]/(the number of MB-SA per mg).

https://doi.org/10.1021/acs.analchem.2c03666
Anal. Chem. XXXX, XXX, XXX−XXX

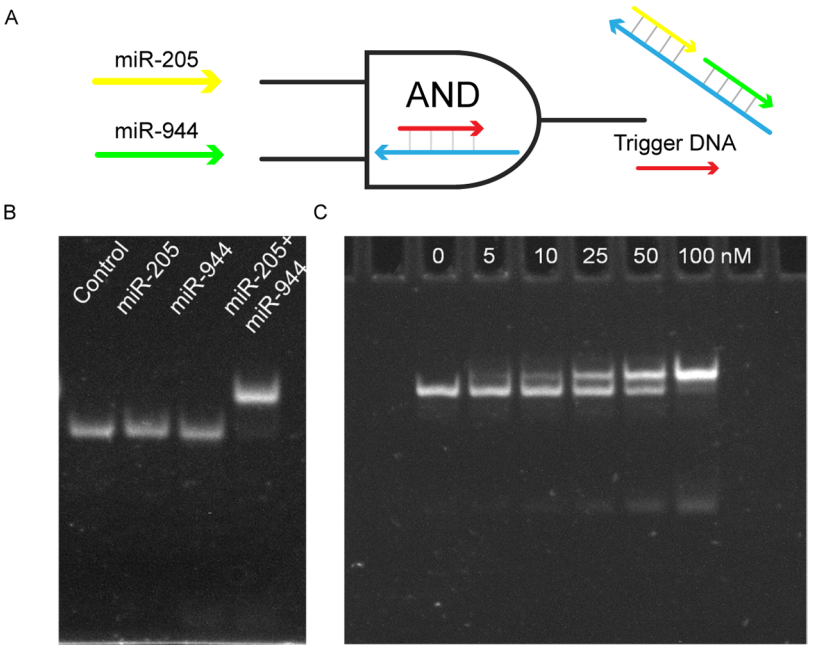


Figure 1. (A) Scheme of DNA computation after DNA probe was incubated with dual miRNAs. (B) Native PAGE image of DNA computation after DNA probe was incubated with dual miRNAs. (C) Native PAGE image of DNA computation after DNA probe was incubated with different concentrations of target miRNAs.

Preparation for Colorimetric Substrate. The colorimetric substrate was prepared by mixing 10 mL of the MES buffer (100 mM, pH 5.7), 100 μL of horseradish peroxidase (1 mg/mL), 40 μL of the TOOS solution (100 mM), 5 μL of the 4-AA solution (10%), and 2 mL of glucose solution (15%).

Verification of the Trans-Cleavage Activity of CRISPR-Cas12a. The trigger DNA was diluted to 1 nM with PBS. One microliter of Cas12a diluent (0.5 μM) was preincubated with 1 μL of crRNA (0.5 μM) to form the CRISPR-Cas12a system. After that, 1 μL of the ssDNA reporter and 20 μL of reaction buffer (20 mM Tris−HCl (pH 7.5), 100 mM KCl, 25 mM $MgCl_2$, and 0.05% Tween 20) were added. Fifty microliters of trigger DNA was incubated with the above mixture for 40 min at 37 °C. To inactivate the CRISPR-Cas12a system, the mixture was further incubated at 75 °C for 10 min. After that, 150 μL of the ultrapure water was added and the fluorescence assay was performed on a fluorescence spectrometer.

Native Polyacrylamide Gel Electrophoresis. Twenty microliters of DNA sample were mixed with 2 μL of DNA loading buffer and then injected into the notch of gel (15%). The gel was run in 1 × TBE buffer for 80 min at a constant voltage of 120 V. After that, the gel was immersed in the GelRed dye solution for 30 min. The image of the gel was obtained by the JS-680D automatic digital gel imaging analysis system.

Detection of miR-944 and miR-205 in Buffer. A solution containing miR-944 and miR-205 was diluted to certain concentrations with PBST. Fifty microliters of the solution was added with 1 μL of the DNA probe-modified MB (10 mg/mL). After incubation at 40 °C for 1 h, the supernatant was obtained via magnetic separation. crRNA and Cas12a were first premixed and then added with 20 μL reaction buffer and 2 μL of GOx-modified MB (10 mg/mL). The mixture was incubated with 50 μL of the obtained supernatant for 1 h. After that, the MB was removed via magnetic separation and the supernatant was taken out. The colorimetric substrate was then added to the supernatant. The colorimetric signal could be read out after incubation at 37 °C for 10 min. Ten microliters of the HCl solution (1 M) could be added to stop the reaction.

Detection of miR-944 and miR-205 in Human Serum. Different concentrations of target miRNAs were spiked into 200 μL of human serum. Afterward, the spiked human serum was treated with a Tiangen RNA extraction kit to obtain the miRNAs. Regarding the real sera of healthy people and lung cancer patients from the hospital, the serum was directly treated with a Tiangen RNA extraction kit to obtain the miRNAs. Twenty-five microliters of the extracted miRNA was diluted to 50 μL with PBST for analysis according to the above-mentioned procedure.

RESULTS AND DISCUSSION

Preparation of DNA Probe for DNA Computation. A partially hybridized DNA probe was rationally designed for dual-miRNA recognition and DNA computation. In the DNA probe, the long-strand DNA was able to pair with miR-944 and miR-205, and the short-strand DNA (trigger DNA) was used to block part of the binding sites of target miRNAs on long-strand DNA. With the input of miR-944 and miR-205, DNA computation was initiated to form the hybrid of the long-strand DNA and target miRNAs and to output the trigger DNA (Figure 1A). By contrast, the single input of miR-944 or miR-205 could not trigger DNA computation. Native polyacrylamide gel electrophoresis (native PAGE) was used to confirm the response of the DNA probe for DNA computation in the presence of dual miRNAs. As shown in Figure 1B, the band of the DNA probe was not changed when miR-944 or miR-205 was lacking. In the presence of both miR-944 and miR-205, the band of the DNA probe almost disappeared and a slowly migrated band emerged, which could be regarded as the hybrid of the long-strand DNA, miR-944 and miR-205. The result confirmed that the DNA probe could

https://doi.org/10.1021/acs.analchem.2c03666
Anal. Chem. XXXX, XXX, XXX−XXX

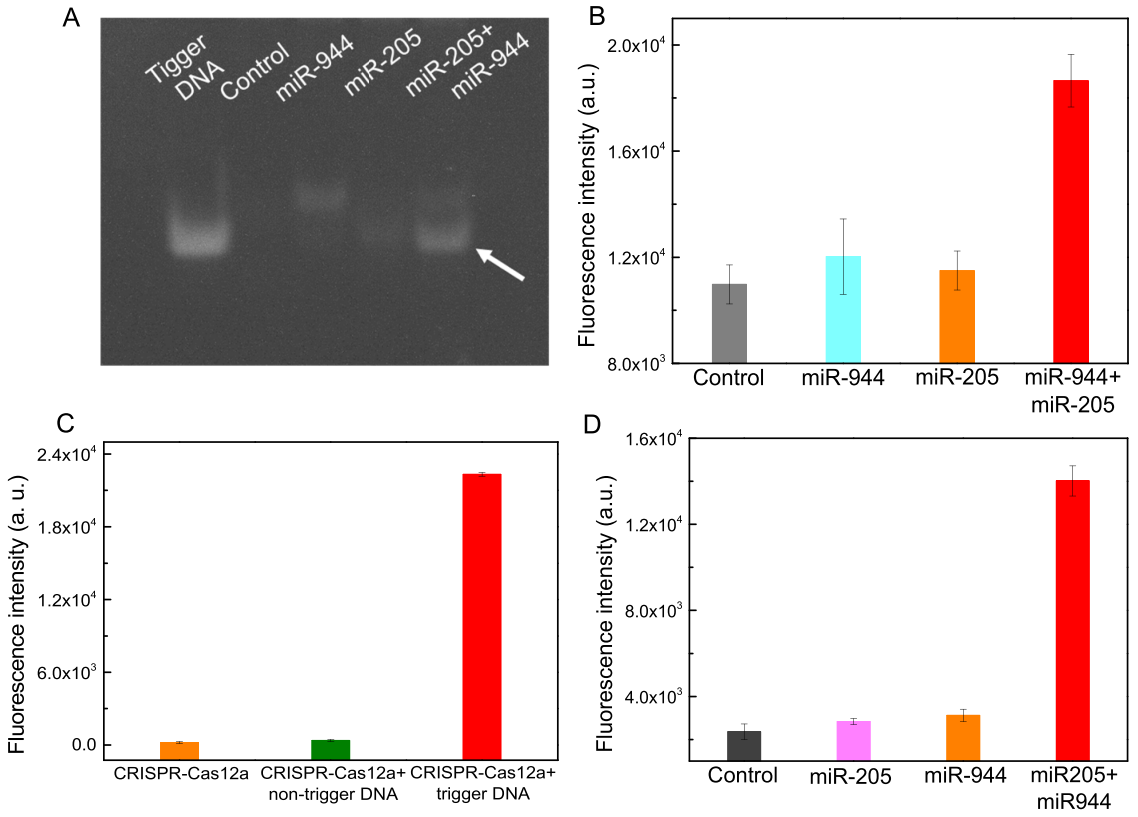


Figure 2. (A) Native PAGE image of the result of DNA computation after the DNA probe-modified MB was incubated with dual miRNAs. (B) Fluorescence recovery after the DNA probe-modified MB was incubated with dual miRNAs. (C) Fluorescence recovery after the trans-cleavage activity of CRISPR-Cas12a was activated by trigger DNA. (D) Fluorescence recovery initiated by the developed strategy in the presence of dual miRNAs.

be successfully utilized for recognizing the dual miRNAs and performing DNA computation. The excess of single miR-944 or miR-205 would not interfere with the response of the DNA probe (Figures S1 and S2). Next, the response of the DNA probe to different concentrations of target miRNAs was studied. As shown in Figure 1C, the band of the hybrid of long-strand DNA and target miRNAs was observed even when the target miRNAs concentration was low compared with that of the DNA probe. Furthermore, the band intensity of the hybrid of long-strand DNA and dual miRNAs was enhanced with the increasing concentration of target miRNAs. The results suggested that the DNA probe performed well with the change in the target miRNA concentration.

Modification of the DNA Probe on MB. It was essential to ensure the hybridization of the long-strand DNA and trigger DNA at a 1:1 molar ratio because little unpaired DNA could influence the detection result, especially when the target miRNA concentration was low. To completely avoid the interference of the unpaired long-strand DNA or trigger DNA for DNA computation, the DNA probe was anchored on the surface of streptavidin-modified MB (MB-SA) based on the affinity of biotin and streptavidin (SA). A certain amount of biotinylated long-strand DNA on MB could be completely blocked by trigger DNA and the redundant trigger DNA was washed away, achieving the isometric hybridization of trigger DNA and long-strand DNA. In addition, the superfluous DNA probe, which might serve as the cleavage substrate of activated CRISPR-Cas12a and influence the detection result, could be removed via magnetic separation after the hybridization reaction. The binding ability of MB-SA for biotinylated DNA was investigated. Figure S3 shows that no DNA band appeared in lane (b) and lane (d), demonstrating that biotinylated DNA with low concentration could be completely bound by MB-SA. The amount of biotinylated DNA conjugated on MB-SA was 0.7 nmol/mg (3.1×10^4 per MB-SA particle) (Figure S4). The DNA probe-modified MB was prepared for use in the subsequent experiments.

Preparation of GOx-Modified MB. The GOx-modified MB (GOx-ssDNA-MB) was synthesized using the previously reported method and utilized for colorimetric signal generation.[40] The ssDNA linker was first linked to GOx via a covalent binding of thiol and maleimide. Figure S5 displays that the migration of thiolated DNA was remarkably restrained when it was conjugated with GOx, which demonstrated the successful preparation of ssDNA-modified GOx (GOx-ssDNA). Afterward, GOx-ssDNA was mixed with MB-SA to form GOx-ssDNA-MB based on the binding of biotin on the terminal of the ssDNA and the SA on MB. As can be seen from Figure S6, the GOx-ssDNA-MB effectively catalyzed the substrate to generate color change, suggesting that GOx was successfully modified on MB via an ssDNA linker. In contrast, almost no change in color was observed after GOx was incubated with MB-SA, proving that the GOx would not be nonspecifically absorbed on MB-SA.

Feasibility of the Developed Strategy for Dual-miRNA Detection. Native PAGE was performed to further confirm the DNA computation on MB. Figure 2A shows that the trigger DNA band emerged after the DNA probe-modified MB was incubated with miR-944 and miR-205. In addition, the terminal of trigger DNA was modified with FAM dye and the

https://doi.org/10.1021/acs.analchem.2c03666
Anal. Chem. XXXX, XXX, XXX−XXX

release of trigger DNA from MB was investigated by fluorescence assay. As displayed in Figures 2B and S7, fluorescence intensity was enhanced only when dual miRNAs were added. Native PAGE assay and fluorescence analysis suggested that target miRNAs could successfully activate DNA computation and replace the trigger DNA from the DNA probe-modified MB. The activation of single-stranded DNase activity of CRISPR-Cas12a by trigger DNA was studied through fluorescence analysis. As shown in Figure 2C, the fluorescence intensity was not changed in the absence of trigger DNA. In comparison, there was an obvious enhancement of fluorescence intensity after the trigger DNA was introduced into the reaction system, demonstrating that the trigger DNA could successfully activate the trans-cleavage activity of the CRISPR-Cas12a system and then lead to the cleavage of the ssDNA reporter. Figure 2D shows that target miRNAs are capable of substituting trigger DNA from the DNA probe-modified MB, causing the collateral cleavage of CRISPR-Cas12a for ssDNA reporter and the generation of enhanced fluorescence intensity. Next, the feasibility of the developed strategy for colorimetric detection of the target miRNAs was investigated. As shown in Figure 3, the input of

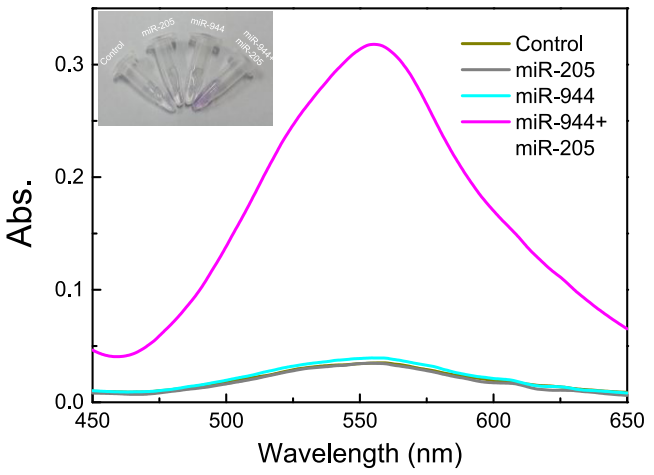


Figure 3. UV−vis absorbance curves of the solution when dual miRNAs were introduced and detected by the developed strategy.

dual miRNAs indeed resulted in the generation of a colorimetric signal, which could be easily distinguished via the naked eye. The result confirmed that the detection of dual miRNAs by the developed strategy was feasible.

Optimization for Experimental Conditions. The optimal reaction conditions were explored to achieve excellent analytical performance. The influence of incubation temperature on DNA computation was studied. As displayed in Figures 4A and S8, the solution color was faint when the incubation temperature was below 30 °C, which might be attributed to the fact that a relatively low temperature affected the hybridization of target miRNAs with DNA probe and thus resulted in the low efficiency of DNA computation. With the increase in incubation temperature, an obvious colorimetric signal emerged. Remarkable purple color could be observed when the incubation temperature was 40 °C. The results suggested that incubation temperature was a significant factor for the generation of a colorimetric signal. Afterward, the incubation time for DNA computation was investigated. Figures 4B and S9 show that the colorimetric signal deepened with the increase in incubation time and changed a little when incubation time exceeded 60 min, demonstrating that 60 min was enough to finish DNA computation and generate a distinct colorimetric signal. In addition, the concentration of CRISPR-Cas12a in the reaction system was also important to realize the ideal detection for target miRNAs. Figures 4C and S10 display that the colorimetric signal was relatively light when the CRISPR-Cas12a concentration was 10 nM. When the concentration of CRISPR-Cas12a reached 25 nM and continued to increase, the color was not significantly changed, suggesting that 25 nM of CRISPR-Cas12a could satisfy the requirement for the target miRNA detection.

Analytical Performance of the Developed Strategy. The analytical performance of the developed strategy was investigated under the optimized conditions. The relationship between the colorimetric signal and the concentration of target miRNAs was explored. As displayed in Figure 5, the solution color gradually turned into obvious purple with an increase in dual-miRNA concentration. To better analyze the relationship between colorimetric signal and target miRNA concentration, the UV−vis absorption of the solution was measured by a UV−vis absorption spectrophotometer. The UV−vis absorption steadily increased when the concentration of target miRNAs was low and significantly enhanced when the concentration was higher than 200 pM. The correlation equation is $Y = 0.03686 \lg X + 0.09623$ ($R^2 = 0.98949$) in the range from 50 fM to 50 pM. The instrumental limit of

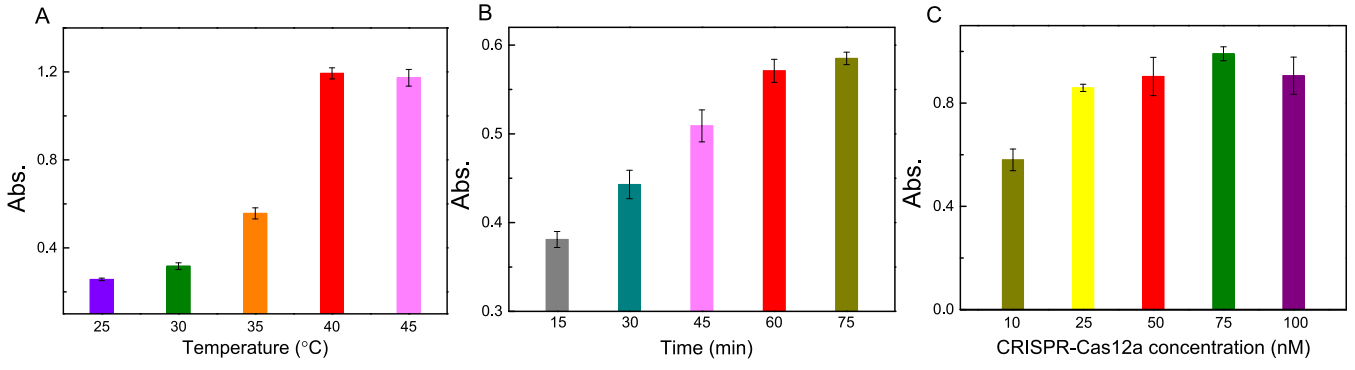


Figure 4. (A) Optimization of incubation temperature of dual miRNAs and the DNA probe-modified MB in the developed strategy. (B) Optimization of incubation time of dual miRNAs and the DNA probe-modified MB in the developed strategy. (C) Optimization of the concentration of CRISPR-Cas12a in the developed strategy.

https://doi.org/10.1021/acs.analchem.2c03666
Anal. Chem. XXXX, XXX, XXX−XXX

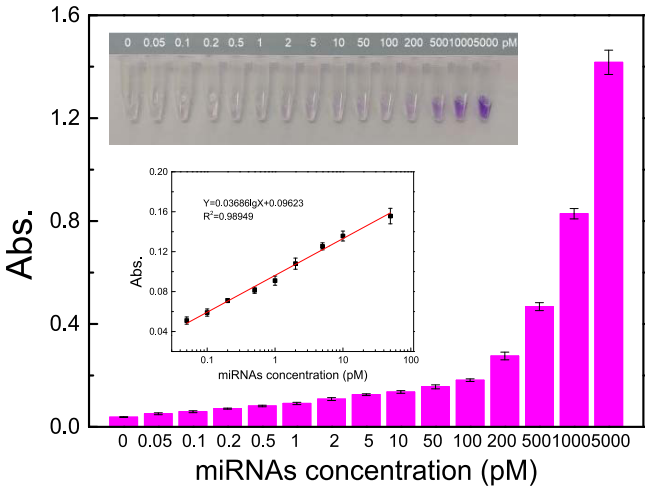


Figure 5. UV−vis absorbance and colorimetric signal change of solution with the increasing concentration of dual miRNAs.

detection (LOD) was calculated to be 36.4 fM (3σ rule), which was approximately 500 folds lower than that reported previously by colorimetric method.[29] In addition, the lowest concentration of target miRNAs that could induce visible colorimetric signal generation was determined to be 1 pM (Figure S11). The results suggested that the developed strategy was sensitive to the detection of dual miRNAs.

Afterward, several other miRNAs, including miR-223, miR-200b, miR-155, and miR-21, were mixed and utilized as an interfering substance to test the detection selectivity of the developed strategy. As can be seen in Figure 6, there was

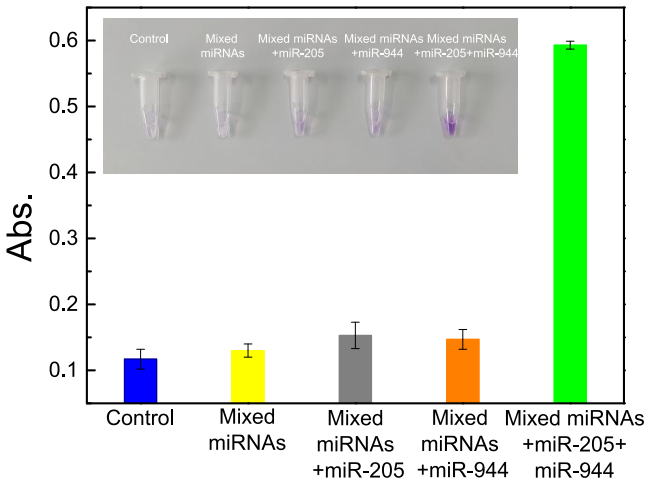


Figure 6. UV−vis absorbance and colorimetric signal change of the solution when dual miRNAs were added. Mixed miRNAs (1 nM of miR-223, miR-200b, miR-21, miR-155).

almost no color change in the group of mixed miRNAs and the control group, suggesting that the interfering miRNAs could not trigger DNA computation and lead to color change. In addition, the input of single miR-944 or miR-205 in the mixture of interfering miRNAs was also not able to generate notable color change. The solution color was changed to remarkable purple only when both miR-944 and miR-205 were added to the mixture. miR-944 and miR-205 with a single-base mutation have been designed to further investigate the analytical specificity. Figure S12 shows that the mutated miR-944 and miR-205 could be successfully distinguished by the color change of the solution. The results demonstrated that the detection selectivity of the developed strategy was satisfactory.

The developed strategy was also applied to detect the miRNAs in the real human serum sample. A certain concentration of target miRNAs was added to human serum, and then the spiked human serum was treated with an miRNA extraction kit to obtain miRNAs, which were subsequently analyzed by the developed strategy. Figure S13 shows that almost no color change was observed when target miRNAs were not spiked in human serum. The solution color gradually deepened with the increase in the target miRNA concentration, proving that the developed strategy could be successfully utilized for detecting miRNAs in human serum. The recovery rates of 50, 300, and 700 pM of target miRNAs were calculated to be 90.55, 92.19, and 86.99%, respectively, based on the calibration curve in Figure S14, which demonstrates that the detection performance of the developed strategy was good (Table 1). The serum of healthy people and

Table 1. Recovery Rate of Different Concentrations of miRNAs Extracted from Human Serum

spiked target miRNAs (pM)	measured concentration (pM)	recovery rate (%)	relative standard deviation (%) (n = 3)
50	45.27	90.55	5.91
300	276.58	92.19	3.49
700	608.93	86.99	2.90

lung cancer patients was collected and treated with an miRNA extraction kit to obtain miRNAs. The miRNAs were then detected by the developed strategy. Figure 7 displays that the

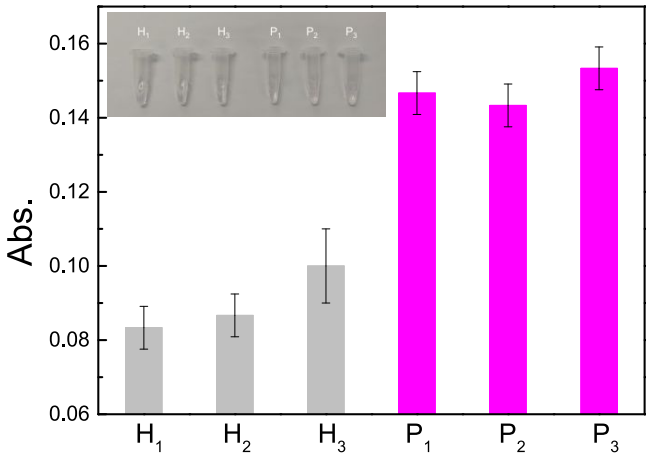


Figure 7. Qualitative analysis of miR-944 and miR-205 in the serum of healthy people (H_1, H_2, H_3) and lung cancer patients (P_1, P_2, P_3).

color change of the solution could be used to distinguish between healthy people and lung cancer patients, suggesting the potential application of the developed strategy for the diagnosis of lung cancer. Reverse transcription-polymerase chain reaction (RT-PCR) as the gold-standard method was also employed to detect miR-205 and miR-944 in the serum of healthy people and lung cancer patients. The results in Figure S15 are consistent with the colorimetric signal in Figure 7, suggesting that the detection reliability of the developed strategy is good.

https://doi.org/10.1021/acs.analchem.2c03666
Anal. Chem. XXXX, XXX, XXX−XXX

CONCLUSIONS

In conclusion, we have developed a sensitive colorimetric strategy that combined AND logic gate and CRISPR-Cas12a system for the simultaneous detection of dual miRNAs. The prepared DNA probe has successfully been used for DNA computation, which output trigger DNA to initiate signal transduction and to generate a visible signal. The visual LOD was 1 pM and the instrumental detection sensitivity was improved by approximately 500 folds compared with previously reported methods. In addition, in the developed strategy, only one kind of crRNA was required to assemble with Cas12a for the detection of dual miRNAs, which simplified the detection procedures and avoided the use of specialized analytical equipment. Healthy people and lung cancer patients could be successfully differentiated using the strategy. The proposed strategy broadens the methodology of CRISPR-Cas12a for in vitro diagnosis and holds great promise for the application of accurate disease diagnosis.

ASSOCIATED CONTENT

Supporting Information

The Supporting Information is available free of charge at https://pubs.acs.org/doi/10.1021/acs.analchem.2c03666.

Reagents and materials; instruments; additional figures as mentioned in the text, including Figures S1−S15; and nucleic acid sequences used in the experiment (PDF)

AUTHOR INFORMATION

Corresponding Authors

Na Li − *College of Chemistry, Chemical Engineering and Materials Science, Key Laboratory of Molecular and Nano Probes, Ministry of Education, Collaborative Innovation Center of Functionalized Probes for Chemical Imaging in Universities of Shandong, Institute of Molecular and Nano Science, Shandong Normal University, Jinan 250014, P. R. China;* orcid.org/0000-0002-0392-6672; Email: lina@sdnu.edu.cn; Fax: (86)-531-86180017

Bo Tang − *College of Chemistry, Chemical Engineering and Materials Science, Key Laboratory of Molecular and Nano Probes, Ministry of Education, Collaborative Innovation Center of Functionalized Probes for Chemical Imaging in Universities of Shandong, Institute of Molecular and Nano Science, Shandong Normal University, Jinan 250014, P. R. China;* orcid.org/0000-0002-8712-7025; Email: tangb@sdnu.edu.cn

Authors

Shaohua Gong − *College of Chemistry, Chemical Engineering and Materials Science, Key Laboratory of Molecular and Nano Probes, Ministry of Education, Collaborative Innovation Center of Functionalized Probes for Chemical Imaging in Universities of Shandong, Institute of Molecular and Nano Science, Shandong Normal University, Jinan 250014, P. R. China*

Xi Wang − *College of Chemistry, Chemical Engineering and Materials Science, Key Laboratory of Molecular and Nano Probes, Ministry of Education, Collaborative Innovation Center of Functionalized Probes for Chemical Imaging in Universities of Shandong, Institute of Molecular and Nano Science, Shandong Normal University, Jinan 250014, P. R. China*

Ping Zhou − *College of Chemistry, Chemical Engineering and Materials Science, Key Laboratory of Molecular and Nano Probes, Ministry of Education, Collaborative Innovation Center of Functionalized Probes for Chemical Imaging in Universities of Shandong, Institute of Molecular and Nano Science, Shandong Normal University, Jinan 250014, P. R. China*

Wei Pan − *College of Chemistry, Chemical Engineering and Materials Science, Key Laboratory of Molecular and Nano Probes, Ministry of Education, Collaborative Innovation Center of Functionalized Probes for Chemical Imaging in Universities of Shandong, Institute of Molecular and Nano Science, Shandong Normal University, Jinan 250014, P. R. China;* orcid.org/0000-0002-2281-8749

Complete contact information is available at: https://pubs.acs.org/10.1021/acs.analchem.2c03666

Notes

The authors declare no competing financial interest.

ACKNOWLEDGMENTS

This work was supported by the National Key R&D Program of China (2019YFA0210100), Shandong Provincial Key Research and Development Program (Major Scientific and Technological Innovation Project) (2021CXGC010515), and Jinan Innovation Team (2021GXRC034).

REFERENCES

(1) Kaminski, M. M.; Abudayyeh, O. O.; Gootenberg, J. S.; Zhang, F.; Collins, J. J. *Nat. Biomed. Eng.* **2021**, *5*, 643−656.
(2) Feng, W.; Newbigging, A. M.; Tao, J.; Cao, Y.; Peng, H.; Le, C.; Wu, J.; Pang, B.; Li, J.; Tyrrell, D. L.; Zhang, H.; Le, X. C. *Chem. Sci.* **2021**, *12*, 4683−4698.
(3) Chertow, D. S. *Science* **2018**, *360*, 381−382.
(4) Dai, Y.; Wu, Y.; Liu, G.; Gooding, J. J. *Angew. Chem., Int. Ed.* **2020**, *132*, 20938−20950.
(5) Chen, J. S.; Ma, E.; Harrington, L. B.; Da Costa, M.; Tian, X.; Palefsky, J. M.; Doudna, J. A. *Science* **2018**, *360*, 436−439.
(6) Zhou, M.; Yin, Y.; Shi, Y.; Huang, Z.; Shi, Y.; Chen, M.; Ke, G.; Zhang, X. B. *Chem. Commun.* **2022**, *58*, 4508−4511.
(7) Chen, S.; Wang, R.; Peng, S.; Xie, S.; Lei, C.; Huang, Y.; Nie, Z. *Chem. Sci.* **2022**, *13*, 2011−2020.
(8) Peng, S.; Tan, Z.; Chen, S.; Lei, C.; Nie, Z. *Chem. Sci.* **2020**, *11*, 7362−7368.
(9) Zhou, T.; Huang, M.; Lin, J.; Huang, R.; Xing, D. *Anal. Chem.* **2021**, *93*, 2038−2044.
(10) Gong, S.; Li, J.; Pan, W.; Li, N.; Tang, B. *Anal. Chem.* **2021**, *93*, 10719−10726.
(11) Shao, N.; Han, X.; Song, Y.; Zhang, P.; Qin, L. *Anal. Chem.* **2019**, *91*, 12384−12391.
(12) Tang, Y.; Qi, L.; Liu, Y.; Guo, L.; Zhao, R.; Yang, M.; Du, Y.; Li, B. *Angew. Chem., Int. Ed.* **2022**, *61*, No. 202115907.
(13) Broughton, J. P.; Deng, X.; Yu, G.; Fasching, C. L.; Servellita, V.; Singh, J.; Miao, X.; Streithorst, J. A.; Granados, A.; Sotomayor-Gonzalez, A.; Zorn, K.; Gopez, A.; Hsu, E.; Gu, W.; Miller, S.; Pan, C. Y.; Guevara, H.; Wadford, D. A.; Chen, J. S.; Chiu, C. Y. *Nat. Biotechnol.* **2020**, *38*, 870−874.
(14) Lu, S.; Tong, X.; Han, Y.; Zhang, K.; Zhang, Y.; Chen, Q.; Duan, J.; Lei, X.; Huang, M.; Qiu, Y.; Zhang, D. Y.; Zhou, X.; Zhang, Y.; Yin, H. *Nat. Biomed. Eng.* **2022**, *6*, 286−297.
(15) Tian, W.; Liu, X.; Wang, G.; Liu, C. *Chem. Commun.* **2020**, *56*, 13445−13448.
(16) Chen, M.; Luo, R.; Li, S.; Li, H.; Qin, Y.; Zhou, D.; Liu, H.; Gong, X.; Chang, J. *Anal. Chem.* **2020**, *92*, 13336−13342.
(17) Ackerman, C. M.; Myhrvold, C.; Thakku, S. G.; Freije, C. A.; Metsky, H. C.; Yang, D. K.; Ye, S. H.; Boehm, C. K.; Kosoko-

Thoroddsen, T. F.; Kehe, J.; Nguyen, T. G.; Carter, A.; Kulesa, A.; Barnes, J. R.; Dugan, V. G.; Hung, D. T.; Blainey, P. C.; Sabeti, P. C. *Nature* **2020**, *582*, 277−282.
(18) Welch, N. L.; Zhu, M.; Hua, C.; Weller, J.; Mirhashemi, M. E.; Nguyen, T. G.; Mantena, S.; Bauer, M. R.; Shaw, B. M.; Ackerman, C. M.; Thakku, S. G.; Tse, M. W.; Kehe, J.; Uwera, M. M.; Eversley, J. S.; Bielwaski, D. A.; McGrath, G.; Braidt, J.; Johnson, J.; Cerrato, F.; Moreno, G. K.; Krasilnikova, L. A.; Petros, B. A.; Gionet, G. L.; King, E.; Huard, R. C.; Jalbert, S. K.; Cleary, M. L.; Fitzgerald, N. A.; Gabriel, S. B.; Gallagher, G. R.; Smole, S. C.; Madoff, L. C.; Brown, C. M.; Keller, M. W.; Wilson, M. M.; Kirby, M. K.; Barnes, J. R.; Park, D. J.; Siddle, K. J.; Happi, C. T.; Hung, D. T.; Springer, M.; MacInnis, B. L.; Lemieux, J. E.; Rosenberg, E.; Branda, J. A.; Blainey, P. C.; Sabeti, P. C.; Myhrvold, C. *Nat. Med.* **2022**, *28*, 1083−1094.
(19) Gootenberg, J. S.; Abudayyeh, O. O.; Kellner, M. J.; Joung, J.; Collins, J. J.; Zhang, F. *Science* **2018**, *360*, 439−444.
(20) Xu, S.; Chang, Y.; Wu, Z.; Li, Y.; Yuan, R.; Chai, Y. *Biosens. Bioelectron.* **2020**, *149*, No. 111848.
(21) Ying, L.; Du, L.; Zou, R.; Shi, L.; Zhang, N.; Jin, J.; Xu, C.; Zhang, F.; Zhu, C.; Wu, J.; Chen, K.; Huang, M.; Wu, Y.; Zhang, Y.; Zheng, W.; Pan, X.; Chen, B.; Lin, A.; Tam, J. K. C.; van Dam, R. M.; Lai, D. T. M.; Chia, K. S.; Zhou, L.; Too, H. P.; Yu, H.; Mao, W.; Su, D. *Proc. Natl. Acad. Sci. U.S.A.* **2020**, *117*, 25036−25042.
(22) Yin, X.; Hou, T.; Huang, B.; Yang, L.; Li, F. *Chem. Commun.* **2019**, *55*, 13705−13708.
(23) Prokup, A.; Hemphill, J.; Deiters, A. *J. Am. Chem. Soc.* **2012**, *134*, 3810−3815.
(24) Li, Y.; Deng, J.; Han, Z.; Liu, C.; Tian, F.; Xu, R.; Han, D.; Zhang, S.; Sun, J. *J. Am. Chem. Soc.* **2021**, *143*, 1290−1295.
(25) Zhou, Z.; Wang, J.; Levine, R. D.; Remacle, F.; Willner, I. *Chem. Sci.* **2021**, *12*, 5473−5483.
(26) Jung, J. K.; Archuleta, C. M.; Alam, K. K.; Lucks, J. B. *Nat. Chem. Biol.* **2022**, *18*, 385−393.
(27) Mi, Y.; Zhao, J.; Chu, H.; Li, Z.; Yu, M.; Li, L. *Anal. Chem.* **2021**, *93*, 2500−2509.
(28) Zhang, C.; Zhao, Y.; Xu, X.; Xu, R.; Li, H.; Teng, X.; Du, Y.; Miao, Y.; Lin, H. C.; Han, D. *Nat. Nanotechnol.* **2020**, *15*, 709−715.
(29) Ma, X.; Chen, X.; Tang, Y.; Yan, R.; Miao, P. *ACS Appl. Mater. Interfaces* **2019**, *11*, 41157−41164.
(30) Yu, S.; Wang, Y.; Jiang, L. P.; Bi, S.; Zhu, J. J. *Anal. Chem.* **2018**, *90*, 4544−4551.
(31) Li, D.; Cheng, W.; Li, Y.; Xu, Y.; Li, X.; Yin, Y.; Ju, H.; Ding, S. *Anal. Chem.* **2016**, *88*, 7500−7506.
(32) Miao, P.; Tang, Y.; Wang, B.; Meng, F. *Anal. Chem.* **2016**, *88*, 7567−7573.
(33) Zeng, D.; Wang, Z.; Meng, Z.; Wang, P.; San, L.; Wang, W.; Aldalbahi, A.; Li, L.; Shen, J.; Mi, X. *ACS Appl. Mater. Interfaces* **2017**, *9*, 24118−24125.
(34) Raitoharju, E.; Lyytikainen, L. P.; Levula, M.; Oksala, N.; Mennander, A.; Tarkka, M.; Klopp, N.; Illig, T.; Kahonen, M.; Karhunen, P. J.; Laaksonen, R.; Lehtimaki, T. *Atherosclerosis* **2011**, *219*, 211−217.
(35) Menghini, R.; Casagrande, V.; Federici, M. *J. Cardiovasc. Trans. Res.* **2013**, *6*, 924−930.
(36) Singh, R. P.; Massachi, I.; Manickavel, S.; Singh, S.; Rao, N. P.; Hasan, S.; Mc Curdy, D. K.; Sharma, S.; Wong, D.; Hahn, B. H.; Rehimi, H. *Autoimmun. Rev.* **2013**, *12*, 1160−1165.
(37) Srivastava, A.; Dixit, A. B.; Banerjee, J.; Tripathi, M.; Sarat Chandra, P. *Clin. Chim. Acta* **2016**, *452*, 1−9.
(38) Li, J.-H.; Sun, S.-S.; Li, N.; Lv, P.; Xie, S.-Y.; Wang, P.-Y. *Oncotarget* **2017**, *8*, 91938−91949.
(39) Powrózek, T.; Krawczyk, P.; Kowalski, D. M.; Winiarczyk, K.; Olszyna-Serementa, M.; Milanowski, J. *Transl. Res.* **2015**, *166*, 315−323.
(40) Gong, S.; Zhang, S.; Wang, X.; Li, J.; Pan, W.; Li, N.; Tang, B. *Anal. Chem.* **2021**, *93*, 15216−15223.

Recommended by ACS

Duplex-Specific Nuclease-Assisted CRISPR-Cas12a Strategy for MicroRNA Detection Using a Personal Glucose Meter
Shaohua Gong, Bo Tang, *et al.*
JULY 19, 2021
ANALYTICAL CHEMISTRY
READ

"Dual-Signal-On" Integrated-Type Biosensor for Portable Detection of miRNA: Cas12a-Induced Photoelectrochemistry and Fluorescence Strategy
Haoran Shen, Weipeng Liu, *et al.*
AUGUST 17, 2021
ANALYTICAL CHEMISTRY
READ

Click Chemistry Actuated Exponential Amplification Reaction Assisted CRISPR–Cas12a for the Electrochemical Detection of MicroRNAs
Hongguo Wei, Jiayu Wan, *et al.*
SEPTEMBER 26, 2022
ACS OMEGA
READ

Integration of the Ligase Chain Reaction with the CRISPR-Cas12a System for Homogeneous, Ultrasensitive, and Visual Detection of microRNA
Xinrong Yan, Yongqiang Cheng, *et al.*
FEBRUARY 23, 2022
ANALYTICAL CHEMISTRY
READ

Get More Suggestions >

https://doi.org/10.1021/acs.analchem.2c03666
Anal. Chem. XXXX, XXX, XXX−XXX